

# ENSO-Monsoon Relationship in a 1000-yr MRI-CGCM Simulation

Akio Kitoh

Meteorological Research Institute, Tsukuba, Ibaraki 305-0052, Japan

Email: kitoh@mri-jma.go.jp

## Abstract

The interannual variability of the Indian summer monsoon rainfall and its close relation with ENSO is known (drought conditions over India accompany warm ENSO events and vice versa), but recent observation suggests a weakening of this ENSO-monsoon relationship and a possible link to global warming is suggested. Here we analyze ENSO-monsoon relationship in a 1000-year control simulation of the MRI coupled GCM (MRI-CGCM2.2). An overall correlation between the JJA Nino3.4 SST and the JJA Indian monsoon rainfall is  $-0.39$  with reasonable circulation characteristics associated with model ENSO. Simulated ENSO-monsoon relationship reveals long-term variations from  $-0.71$  to  $+0.07$  in moving 31-year windows. In the first 500 years, the model shows a slight warming with a temporary weakening of the thermohaline circulation and its recovery. In this period the ENSO-monsoon relationship collapses when northern high-latitudes are warm, suggesting a larger temperature contrast between land and ocean being responsible for a weaker ENSO-monsoon relationship. In the latter 500 years of the integration when thermohaline circulation and global mean surface air temperature is stable, ENSO-monsoon relationship becomes large when tropical interannual variability is large.

*Keyword: ENSO, monsoon, decadal variability, global warming, GCM*

## 1. Introduction

It is well known that the Indian summer (June-September) monsoon rainfall (IMR) becomes below normal in El Niño years and becomes above normal in La Niña years. This negative correlation between the sea surface temperature (SST) anomalies over the equatorial central/eastern Pacific and the IMR is called the ENSO-monsoon relationship.

However this relationship, although statistically significant over the available long-term observed record, shows a decadal fluctuation and even shows a collapse in the relationship in recent years (e.g. Krishna Kumar et al. 1999). Many hypotheses are raised on this recent collapse of the ENSO-monsoon relationship, such as decadal variability (Kripalani and Kulkarni 1997), change in seasonality of ENSO cycle (Kawamura et al. 2003), Indian Ocean Dipole mode (Ashok et al. 2001), Atlantic Oscillation (Chang et al. 2001) and global warming. With respect to the global warming, continental warming (Krishna Kumar et al. 1999) or Walker circulation change (Ashrit et al. 2001) can be candidates for the reason.

For the general circulation model (GCM) results, Ashrit et al. (2001, 2002) analyzed the MPI and CNRM model output and showed a large natural variability. On the other hand, the MRI model showed a decrease in the ENSO-monsoon relationship under global warming with asymmetric features between El Niño and La Niña: El Niño-weak IMR relationship becomes weak but La Niña-strong IMR relationship does not change (Ashrit et al. 2004).

In this study, we analyze the ENSO-monsoon relationship and its long-term variability in the 1000-year integration of the MRI coupled GCM. This model (MRI-CGCM2: Yukimoto et al. 2001) has shown an ability to reproduce a reasonable climate without flux adjustments (Kitoh 2004).

## 2. Model Climate

We used a version of the Meteorological Research Institute global atmosphere-ocean coupled GCM (MRI CGCM2, Yukimoto et al. 2001). The model consists of a T42 L30 AGCM and a global  $0.5$ - $2.0^\circ$  by  $2.5^\circ$  L23 OGCM. The initial condition comes from the previous flux-adjusted model simulation. This model has been integrated for 1000 years without flux adjustments.

Figure 1 shows the 1000-year time series of the global and annual mean surface air temperature and the strength of the Atlantic thermohaline circulation. At the beginning, the flux adjustment was turned off, and the surface air temperature slightly rises about  $0.9^\circ\text{C}$  in the first 500 years. The Atlantic thermohaline circulation initially drops from 19 Sv to 16 Sv, but afterwards it recovers in several hundred years. The strength in the last 500 year mean is about 17.7 Sv.

Figure 2 shows the June-August (JJA) mean SST and precipitation averaged for years 901–1000. The model reproduces climatological SST and precipitation distributions reasonably well. Although the model tends to show a double ITCZ structure in the tropical eastern Pacific, the Asian monsoon precipitation is simulated very well (Kitoh 2004).

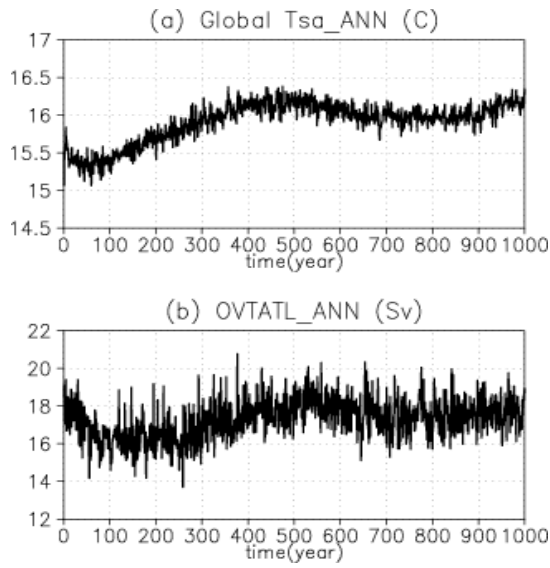


Figure 1. 1000-year time series of (a) annual and global mean surface air temperature ( $^{\circ}\text{C}$ ) and (b) strength of the Atlantic thermohaline circulation (Sv).

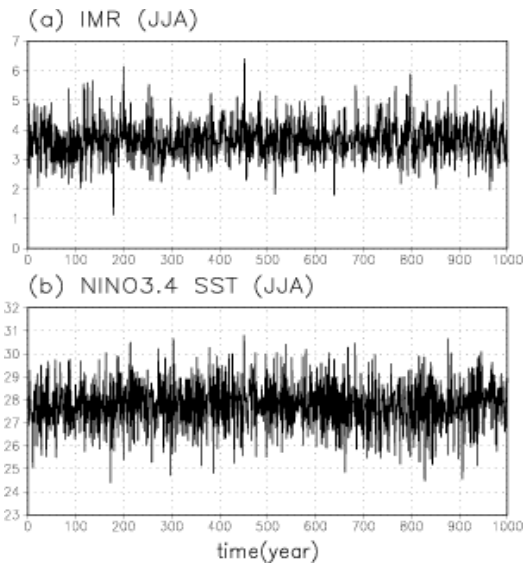


Figure 3. 1000-year time series of (a) JJA mean precipitation over India (IMR) (mm/day) and (b) JJA mean NINO3.4 SST ( $^{\circ}\text{C}$ ).

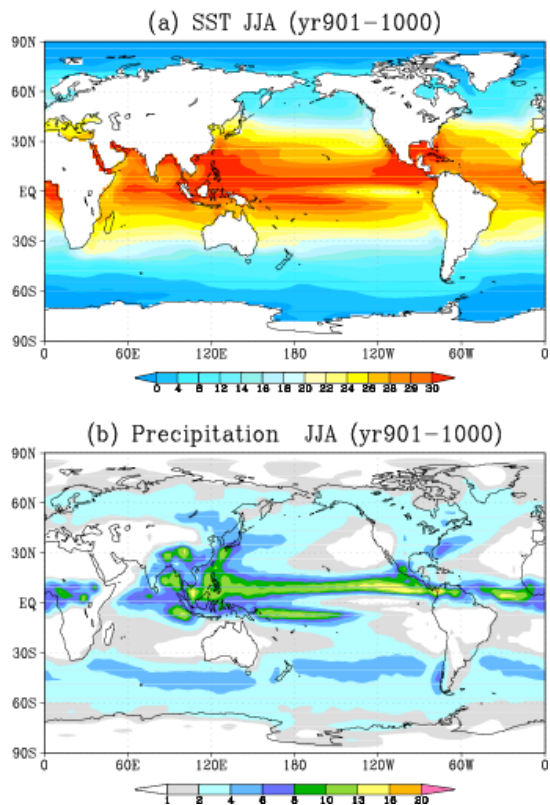


Figure 2. (a) JJA mean SST and (b) JJA mean precipitation averaged for year 901-1000.

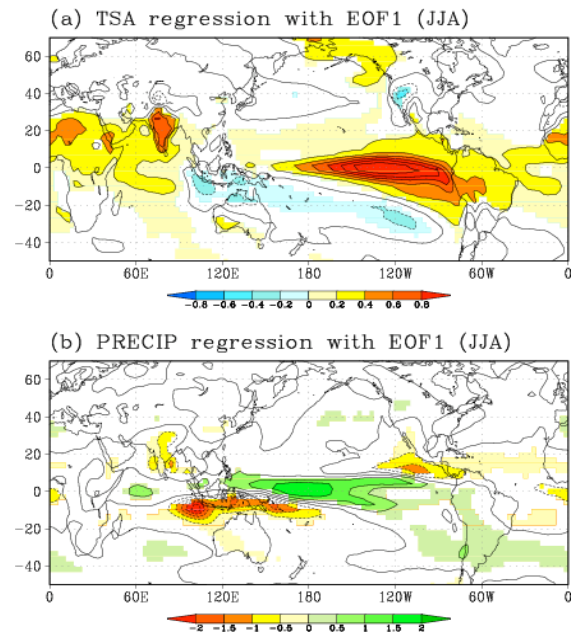


Figure 4. Regression fields of the (a) surface air temperature and (b) precipitation in JJA on the first EOF of the near global SST of the 1000-year integration in JJA.

### 3. Model ENSO

The model reproduces a reasonable El Niño and associated precipitation and atmospheric circulation changes. Figure 3 shows a 1000-year time-series of IMR and Nino3.4 SST in JJA. Correlation coefficient between them is  $-0.39$ . Therefore the model shows a significant negative correlation between IMR and Nino3.4 SST. Figure 4 shows the regressions of the JJA surface air temperature and precipitation on the leading EOF mode of the near global SST. There are positive SST anomalies over the equatorial central and eastern Pacific, the Indian Ocean and the Atlantic Ocean. Negative SST anomalies are found over the western tropical Pacific. The eastern equatorial Indian Ocean is also covered by negative SST anomalies. Large precipitation anomalies are associated with the SST anomalies in the tropical Pacific and the Indian Ocean, implying an eastward displacement of the rainfall center. It is noted that negative precipitation anomalies are noted over India associated with model El Niño.

### 4. Evolution of ENSO-Monsoon relationship

In this section, we describe the temporal variability of the simulated ENSO-monsoon relationship. Figure 5 shows the 31-year sliding correlations between IMR and NINO3.4 SST anomalies in JJA during the 1000-year simulation. The correlation coefficient shows a large interdecadal variability and varies between  $-0.71$  and  $+0.07$ . There are periods with large negative correlations (strong ENSO-monsoon relationship), such as decades 90s, 350s and 940s, and periods with almost no correlation, such as 470s, 560s and 910s.

In order to capture any simultaneous/precursor signals of IMR variability, lagged regression analysis is performed between the time series of Fig. 5 and various variables in simultaneous (JJA) as well as those in one season before (March-May) and two seasons before (December-February). Figure 6 shows the regression fields of surface air temperature anomalies in March-May (MAM) on the time series of 31-year sliding correlations between IMR and NINO3.4 SST anomalies in JJA. It is noted that there are large positive temperature anomalies over northern high latitudes, particularly over the oceans. These features suggest that warmer Eurasian continent in winter and spring leads to stronger continent-to-ocean temperature contrast and thus stronger summer monsoon. The strong summer monsoon itself would not be affected much by the ENSO-related Walker circulation anomalies, thus leading to weaker ENSO-monsoon relationship.

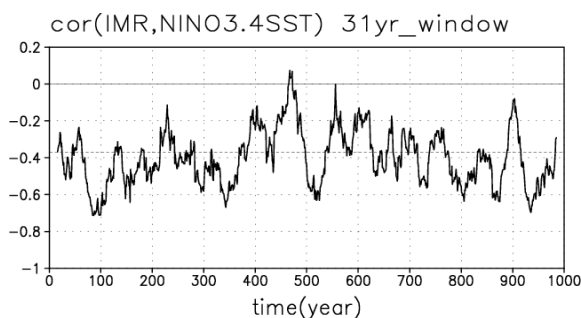


Figure 5. 31-year sliding correlations between IMR and NINO3.4 SST anomalies (JJA) during the 1000-year simulation.

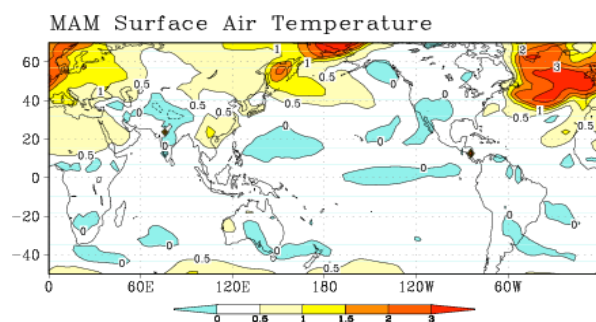


Figure 6. Regression fields of surface air temperature in March-May (MAM) on the time series of 31-year sliding correlations between IMR and NINO3.4 SST anomalies in JJA (Fig. 5).

Figure 7a and b shows the time series of the 31-year sliding mean of IMR and NINO3.4 SST. The 31-year mean IMR varies between 3.29 and 3.94 mm/day, while 31-year mean NINO3.4 SST varies between 27.4 and 28.2°C. Figure 7c and d shows the time series of interannual standard deviations of IMR anomalies and NINO3.4 SST anomalies during respective 31-year sliding window. They also show decadal fluctuations with a factor of two.

Correlations between these indices and the time series of 31-year sliding correlations between IMR and NINO3.4 SST anomalies in JJA are calculated (Table 1) for the entire 1000-year and the first and last 500 year periods. There is a drastic difference between the first and the last 500 year periods. In the first half period, correlation is large in the 31-year sliding mean IMD and NINO3.4 SST. But correlation with global mean surface air temperature is also large, and this may reflect a slight warming ( $0.9^{\circ}\text{C}/500$  years) trend, which

resembles a global warming experiment. With this very long-term trend, the ENSO-monsoon relationship becomes weaker as global temperature as well as monsoon itself becomes stronger. On the other hand, in the latter half period, the ENSO-monsoon relationship is well correlated with the interannual variability of both the NINO3.4 SST and IMR, thus suggesting that decadal-scale variability of the ocean-atmosphere system can influence the ENSO-monsoon relationship. It is noted that the ENSO-monsoon relationship can become small even with this internal variability such as a period of 910s. Mechanism of this decadal variability should be investigated further.

## References

- Ashok et al., *GRL*, **28**, 4499-4502, 2001.  
 Ashrit et al., *GRL*, **28**, 1727-1730, 2001.  
 Ashrit et al., *JMSJ*, **81**, 779-803, 2003.  
 Ashrit et al. (Submitted to *JMSJ*)  
 Chang et al., *JC*, **14**, 2376-2380, 2001.  
 Kawamura et al., *JMSJ*, **81**, 1329-1352, 2003.  
 Kitoh, *JC*, **17**, 783-802, 2004.  
 Kripalani and Kulkarni, *Int.J.Climatol.*, **17**, 1155-1168, 1997.  
 Krishna Kumar et al., *Science*, **284**, 2156-2159, 1999.  
 Rajendran et al., *JC*, **17**, 763-782, 2004.  
 Yukimoto et al. *Pap. Meteor. Geophys.*, **51**, 47-88.

Table 1 Correlation coefficients between several indices and the time series of 31-year sliding correlations between IMR and NINO3.4 SST anomalies in JJA for the entire 1000 years and first and last 500 year period.

indices	Year 1-1000	year 1-500	year 501-1000
Global mean surface air temperature	+0.25	+0.48	-0.14
Atlantic thermohaline circulation	+0.15	+0.29	+0.04
31-year mean IMR	+0.33	+0.49	+0.04
31-year mean NINO3.4 SST	+0.18	+0.48	-0.06
$\sigma$ (IMR) during 31yr window	-0.20	-0.08	-0.42
$\sigma$ (NINO3.4 SST) during 31yr window	-0.21	+0.01	-0.41

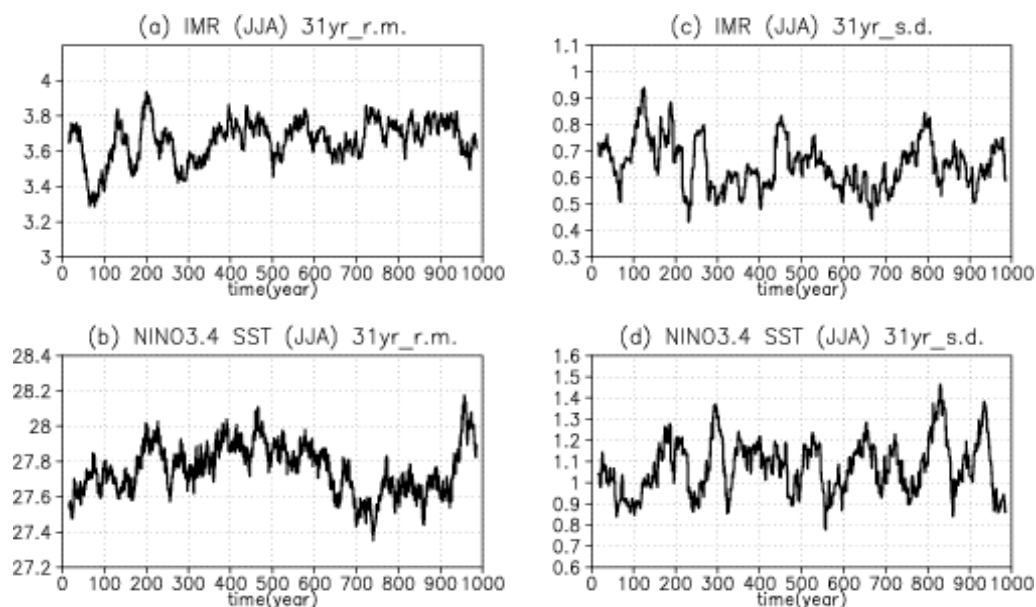


Figure 7. (a) 31-year sliding mean of IMR. (b) 31-year sliding mean of NINO3.4 SST. (c) interannual standard deviation of IMR anomalies during 31-year sliding window. (d) interannual standard deviation of NINO3.4 SST anomalies during 31-year sliding window.